JOURNAL OF MATERIALS SCIENCE **35** (2000) 5829–5837

A model for the large-strain deformation of polyethylene

S. J. K. RITCHIE
School of Engineering and Computer Science, Department of Engineering, Exeter University, EX4 4QF, UK
E-mail: s.ritchie@ex.ac.uk

A model for the large strain deformation of polyethylene under uni-axial tension is described. Based on observations made by other researchers, the model describes hardening at large strains by considering dislocation nucleation and reorientation of slip planes within the crystalline phase. The temperature and strain-rate sensitivity of this behaviour are predicted with reasonable accuracy in a pipe-grade high-density polyethylene. The model has only three adjustable parameters which are the crystal shear modulus, the Young's modulus and a critical dislocation length.

1. Introduction

The plastic deformation of polyethylene to large strains under uni-axial tension and shear appears to control the brittle-tough transition temperature observed in rapid crack propagation of polyethylene [1]. The large strain behaviour of polymers when subjected to uni-axial tension is complicated by necking and cold-drawing [2] and is sensitive to strain-rate and temperature [2]. It is only relatively recently that experimental techniques have been devised to overcome these problems in order to obtain true stress-strain curves at constant true strain-rates [2, 3]. This paper examines the true stress, true strain curves, obtained at constant temperature and true strain-rate, of a pipe-grade high-density polyethylene copolymer reported by Hillmansen *et al.* [4]. The characteristic shape of these curves is an initial linear region followed by yield at a true strain of approximately 0.1 (Figs 1 and 2). After yield a pronounced hardening is observed.

The primary aim of this work is the development of a constitutive elastic-viscoplastic relationship, which can be incorporated into a numerical structural analysis. The model must allow constitutive relations calibrated from low strain-rate experiments to be extrapolated to higher strain rates, where isothermal conditions cannot be maintained due to the high rate of heat generation from the plastic deformation. A reliable system of extrapolation requires consideration of the microstructural mechanisms involved. The model should therefore also provide a framework for examining the effects of processing conditions by providing a link between microstructural parameters, such as lamellar thickness, and mechanical behaviour.

A material model developed by Haward and Thackray [5] attributes the hardening to a decrease in entropy associated with chain reorientation. They used rubber elasticity theory to predict the change in entropy as a function of stretch (λ). The model was originally developed for glassy polymers, and a form of it has been adopted by Boyce *et al.* [6]. Rubber elasticity models, whether developed using a Gaussian or Langevin formulation for chain extension [7], show a stiffening behaviour qualitatively similar to that seen in Figs 1 and 2 in which the stress increases as approximately λ^2. G'Sell and Jonas [8] and Haward [9] have shown that the Gaussian formulation fits such data reasonably well. However, the use of rubber elasticity to model polyethylene deformation below the melt temperature is questionable. As early as 1951 Crawford and Kolsky [10] used birefringence results from drawn polyethylene to show that the molecular reorientation during extension does not even qualitatively follow rubber elasticity theory (Fig. 3).

In addition, rubber elasticity theory does not directly explain the rate or temperature dependence seen in Figs 1 and 2. The stiffness of an ideal rubber actually increases with temperature and is insensitive to strain-rate. Although entropic rubber elasticity undoubtedly has a role to play in the deformation of the amorphous phase it is not yet included in this model. In fact, the model is formulated using only the bare minimum of physical processes ascribed to polyethylene in the literature.

The basic concepts behind the model can be summarised as follows:

- The shear stress acting on crystallographic planes can be resolved at a microstructural level using continuum mechanics.
- The reorientation of the crystallographic planes can be described by the pseudo-affine model of Crawford and Kolsky [10]. The statistical approach to describe distribution of orientations will allow realistic solution times when the model is incorporated into a numerical structural analysis code.

0022–2461

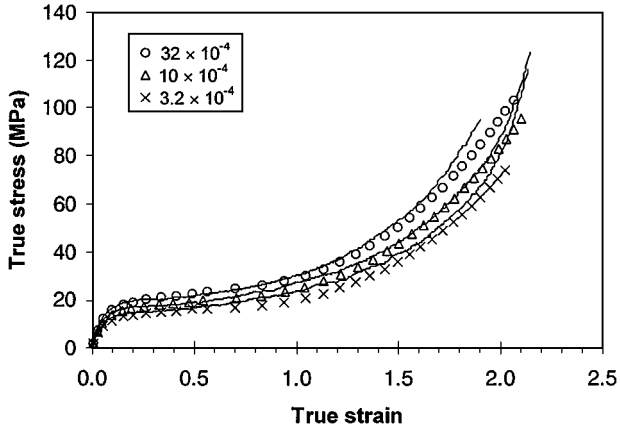

Figure 1 True stress-true strain curves as a function of strain-rate (in. s^{-1}) for a 62% crystalline polyethylene at 46°C [4]. Continuous line: experiment, points: predicted.

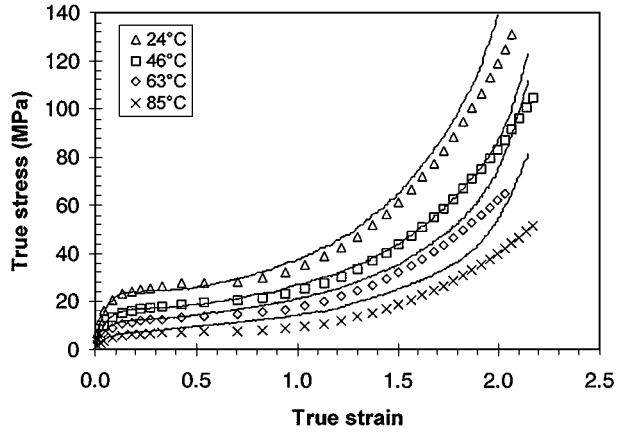

Figure 2 True stress-true strain curves as a function of temperature for a PE100 at a true strain-rate of 10^{-3}/s [4]. Continuous line: experiment, points: predicted.

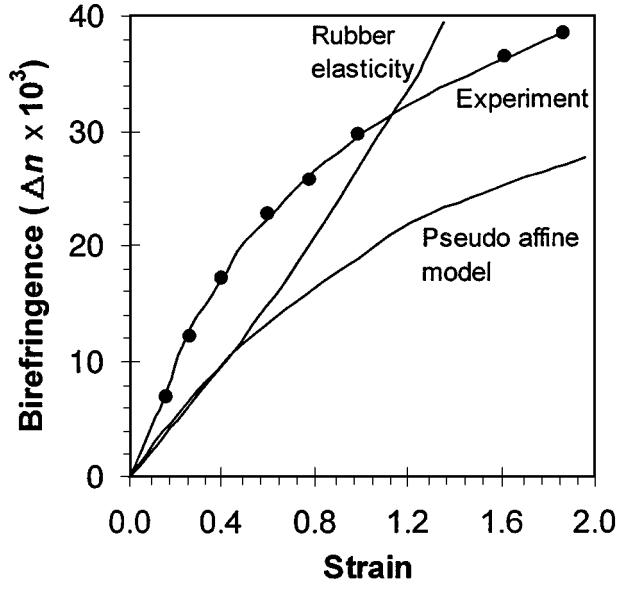

Figure 3 Comparison of predicted and experimental birefringence (Δn) as a function of strain [10]. (Δn increases with chain alignment to the draw direction).

- Yield and post-yield deformation are governed by a thermally activated dislocation nucleation process.
- The combined effect of the all slip planes within the material can be calculated by summing them as if they acted in parallel.

For uni-axial tension the resolved shear stress is calculated, by continuum mechanics, to be at a maximum on planes inclined at $\pm 45^\circ$ to the draw direction. The shear stress then falls to zero on planes aligned parallel or perpendicular to the draw direction. As the material is stretched, reorientation causes the slip planes to become aligned to the draw direction. An increasing true stress in the direction of loading is then required to maintain the same resolved shear stress and rate of slip. The following sections quantify this behaviour to explain the characteristic hardening of the true stress-strain relationship for polyethylene and its temperature and strain-rate dependence.

A similar form of model has been proposed by Ahzi *et al.* [11] (see also G'Sell and Dahoun [12]). They have concentrated on predicting the evolution of crystalline texture with strain rather than the dependence of experimental stress-stretch curves on temperature and strain-rate. The model presented here differs by directly implementing a pseudo-affine deformation law to predict reorientation and using an alternative model for crystalline slip that is directly dependent on microstructural parameters. Ahzi *et al.* used an adapted Taylor model [13] to predict reorientation allowing the dependence on all possible slip systems to be accounted for. In comparison, the pseudo-affine deformation law, as used here, accounts only for the dominant chain slip system. However, the Taylor model does itself make the assumption of affine deformation, with each crystal subjected to the same strain and strain-rate as the polycrystal aggregate.

The next section concentrates on the re-orientation behaviour. The following sections then examine previous research to form a foundation for further assumptions made in the model. An Eyring activation process is then used to model slip within the crystalline phase of the material. The equations derived for the re-orientation and slip mechanisms are finally combined to predict true stress-strain curves which are compared with experiment.

2. Re-orientation due to drawing

As polyethylene is extended the average chain direction becomes aligned to the direction of elongation (z axis). As mentioned above, Crawford and Kolsky showed that the change in birefringence due to this orientation could be predicted using a 'pseudo-affine' model. Their model assumed that chains rotate under the global strain in an affine manner: the change in orientation of any chain segments parallel to a line drawn within the material ($\overline{AB}$ in Fig. 4) would follow that of the drawn line.

Since orientation is a three dimensional property they considered the minimum volume cylinder which lay parallel to the z axis and fully enclosed the line. Considering the extension of this cylinder at constant volume they calculated:

$$\tan(\theta) = \lambda^{-\frac{3}{2}} \tan(\theta_0)$$

where θ is the angle of inclination of a chain segment to the draw direction at a stretch of λ. The angle θ_0

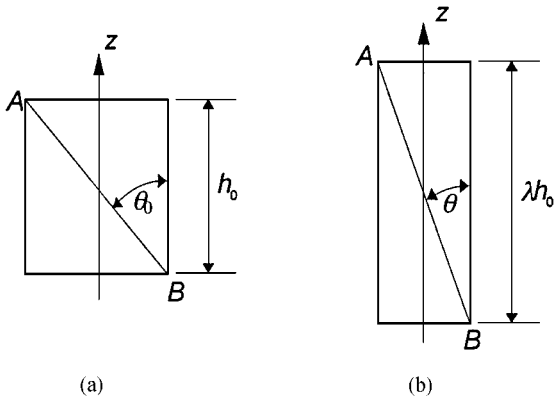

Figure 4 Rotation of a chain segment.

is the initial inclination of the chain segment in the undeformed state ($\lambda = 1$). The model is termed pseudo-affine, as opposed to affine, because the change in length of $\overline{AB}$ is ignored. The number of chain segments (β) per radian inclination is then found to be:

$$\beta = \beta_0 \frac{\lambda^{\frac{3}{2}}}{1 + (\lambda^3 - 1)\sin^2(\theta)} \tag{1}$$

where β_0 is the distribution in the undeformed state.

Assuming a purely random initial distribution [14] gives:

$$\beta_0 = \frac{M}{2}\sin(\theta_0) \tag{2}$$

Where M is the total number of chain segments. The above equations were then used to predict the birefringence as a function of stretch and compared against experimental results (Fig. 3). Crawford and Kolsky considered that the quantitative birefringence error between their pseudo-affine model and experiment might have been due to ignoring the amorphous region. This would indeed affect their analysis of how the light is refracted and their final results, but would not necessarily invalidate Equations 1 and 2. Later, Maxwell *et al.* [15] found good quantitative agreement between the pseudo-affine model and results from wide angle X-ray scattering (although they did find a small variation with crystallinity) and Bartczak *et al.* [16] showed that re-orientation of the amorphous and crystalline phases occurred almost in parallel, the amorphous phase leading by only a few degrees. These results imply that, although the refraction analysis of Crawford and Kolsky was in error, Equations 1 and 2 are valid.

The overall picture is therefore that reorientation of the amorphous and crystalline regions are intimately linked and can be quantitatively modelled by Equations 1 and 2.

3. Intimacy of the amorphous and crystalline phases

The ability of continuum mechanics to accurately resolve shear stresses on crystallographic planes depends on the amorphous and crystalline phases being intimately connected. 'Tie chains' and inter-crystalline links have been proposed as structures which transmit stress between lamellae [17]. The remaining amorphous material is then seen as having little influence on mechanical properties. Tie chains and inter-crystalline links would produce stress concentrations within the lamellae at their points of attachment, making it difficult to resolve shear stresses accurately. Since the slip process proposed in the present model depends on an intimate connection between the phases, this topic is now discussed.

Vadimsky *et al.* [18] used electron microscopy to demonstrate that inextensible crystalline links can exist in the bulk material. However, they also showed that stress can be transmitted on a much finer scale by chains which do not immediately re-enter the lamellae adjacent to the point from which they left it, as they do in regular chain folding. These chains enter the entangled amorphous region and can either re-enter the same lamella at a remote point, enter another lamella or terminate. This idea is supported by Flory and Yoon [19] who, on the basis of a crystal growth rates and neutron scattering experiments, argued that entanglements existing in the melt cannot be undone during crystallisation but become concentrated in the amorphous phase. The process restricts ordered, adjacent re-entry chain folding, making random re-entry far more probable. Adjacent re-entry is further limited in branched polyethylenes since the branches are segregated into the amorphous phase [20, 21]. The argument against significant adjacent re-entry chain folding has been supported more recently by Schönherr *et al.* [22], who examined specimens deformed under plane strain compression by using atomic force microscopy and small angle X-ray scattering.

The picture is therefore one in which molecular chains weave through an entangled amorphous phase, enter lamellae and then pass back into the amorphous phase without showing significant adjacent re-entry. This process is repeated for the complete length of each molecular chain such that each one is included in many lamellae.

For polyethylene to possess the strength and stiffness which it has, the amorphous regions must transmit stress between lamellae without showing excessively high strains [22]. Rubber elasticity theory, which is applicable to the amorphous region above its glass transition temperature ($\approx -70^\circ$C), would suggest high strains. However, the essentially lamellar structure of the crystalline phase suppresses volume contraction of the interlamellar amorphous layers bonded to it, increasing their stiffness to the bulk modulus [23], about 1 GPa. Under these conditions inter-lamellar shear is more likely to dominate the deformation [16, 24].

4. Crystallographic slip

This section describes a mechanism by which the dominant chain slip system is controlled by dislocation nucleation. The dynamics of the slip process are then quantified using the thermal activation process proposed by Krausz and Eyring [25] and commonly used to describe the yield point of polymers [26]. Finally, the relationship between microstructural slip and macroscopic strain is examined with reference to lamellar orientation.

4.1. Dislocation nucleation

It has been established that the dominant plastic deformation mechanism of the crystalline phase is fine chain slip since molecular chains become orientated towards the tensile direction. Transverse slip is also possible and Martensitic transformations can occur, but on a negligible scale [27–29]. The dominance of these mechanisms is due to the high carbon-carbon bond stiffness with respect to that of the Van der Waals bonds.

Chain slip is the slip of one chain over another in the chain direction [001], the slip plane being of the {*h*,*k*,0} type. Due to the trans conformation of the chain the Burgers vector, *b*, is equal to twice the spacing of carbon atoms along the molecular chain (0.254 nm). Only screw dislocations will be considered here since they offer much lower resistance than edge dislocations [30] and their glide is not limited to a specific plane, as with edge dislocations. Screw dislocations along the chain direction have the lowest line energy on the (100) and (010) planes with evidence that slip on the (100) plane is easiest [31]. In order to achieve a model that can realistically be incorporated in a numerical analysis code no distinction is made between the plastic resistances along {*h*,*k*,0} planes. The simplification is supported by the work of Gleiter and Argon [32].

Dislocation theories developed for metals consider homogenous nucleation to be unrealistic and the dislocation density to be maintained by regenerative multiplication of Frank-Read type sources. The lamellae of HDPE are in the order of 20 nm thick [33] and in such thin crystals Frank-Read sources become less viable. Peterson [34] proposed that screw dislocations could be nucleated from the free lateral surfaces of a lamella. Recently Lin and Argon [35] supported the mechanism as possibly playing a governing role. A form of Peterson's analysis is adopted in this model and developed below.

Consider an infinitely thick lamella with a screw dislocation which has nucleated at the edge and moved a distance *l* into the lamella (Fig. 5). The elastic energy of the dislocation per unit length, $E(l)$, is then given by [36]:

$$E(l) = \frac{\mu b^2}{4\pi} \ln\left(\frac{2l}{r_0}\right) \tag{3}$$

where r_0 is the core radius and μ is the crystalline shear modulus, C_{44}. In reality the value of $E(l)$ will actually show a limiting value of approximately $1/2\mu b^2$ but this does not affect the analysis since we are only concerned with small values of l (see below). The analysis suggested by Peterson was aimed at determining a lower bound limit to examine whether dislocation nucleation was a viable system in semi-crystalline polymers. Peterson used a derivation by Eshelby and Stroh [37] to account for the finite thickness of lamellae which is developed from assuming that the lamellar surface planes (001) are stress free. However, the stress free assumption is incorrect if there is an intimate link with the amorphous phase at the (001) surface plane. Furthermore, if $d, l \gg r_0$ then Peterson's lower limit estimation reduces to the same form given in Equation 3 with the factor of 2 in the log term reducing to unity. In this model l is treated as a calibration parameter and therefore Equation 3 may be used, providing the derived values of μ are not taken as being indicative of the theoretical crystal shear modulus. (Young [33] fitted Peterson's model to experimental results by adjusting r_0).

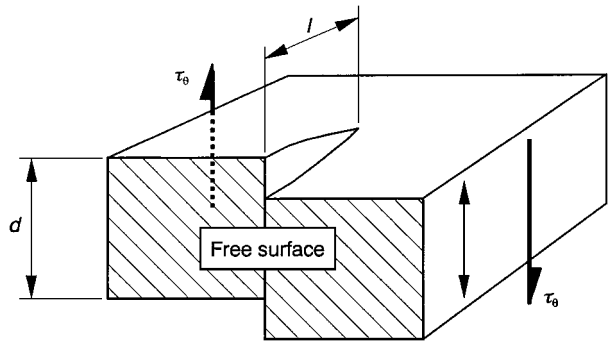

Figure 5 Portion of a lamellar enclosing a screw dislocation at a distance l from the free surface.

The increase in free enthalpy associated with creation of a dislocation from a free edge is therefore:

$$\Delta G(l) = \frac{\mu b^2 d}{4\pi} \ln\left(\frac{2l}{r_0}\right) - \tau_\theta \, dlb \tag{4}$$

where d is the lamellar thickness and τ_θ is the maximum resolved shear stress acting in the [001] direction. Differentiating with respect to l gives the maximum in free enthalpy, $\Delta G_{\max}$, at:

$$l_c = \frac{1}{4\pi} \frac{\mu}{\tau_\theta} b, \text{ which gives}$$

$$\Delta G_{\max} = \frac{\mu b^2 d}{4\pi} \left[\ln\left(\frac{2l_c}{r_0}\right) - 1 \right] \tag{5}$$

To nucleate a screw dislocation in the absence of any thermal energy gives $l_c = 1.4b$, assuming that $r_0 = b$. Young [33] found the average shear modulus of HDPE to be 1 GPa at a strain-rate of order 10^{-3} and the shear stress on preferentially oriented lamellae to be 20 MPa at yield, giving $l_c = 4b$. Due to l_c approaching the assumed size of r_0 the accuracy of Equation 4 is somewhat dubious but the predicted dependence of $\Delta G_{\max}$ on d, b and μ should still hold true.

If Equation 4 were to be believed it would imply that the strain-rate was directly proportional to τ_θ, rather than $\exp(\tau_\theta)$ as experiment shows it to be. Given this fact and that l_c is of the same order of size as r_0, Equation 4 is used, with a value of l_c which is assumed to be stress independent:

$$\Delta G_{\max}(l) = \frac{\mu b^2 d}{4\pi} \ln(2l^*) - \tau_\theta \, db^2 l^* \tag{6}$$

where $l^* = \frac{l_c}{r_0}$ and a value of b is taken for r_0.

Using a drag coefficient analysis [38] gives the velocity, v, of a dislocation once nucleated as approximately:

$$v = \frac{\Omega(\tau_\theta - \tau_p)}{kT} v_s,$$

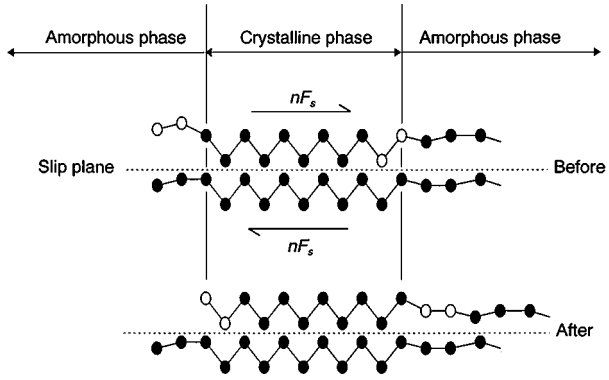

Figure 6 Slip of partial chains across a slip plane. The unfilled circles represent CH_2 units which change phase.

where Ω is the atomic volume, k is the Boltzmann constant, $v_s = \sqrt{\mu/\rho_c}$ is the shear wave speed in the crystal of density ρ_c and τ_p is the Peierls stress which will be negligible relative to τ_θ. Using Young's data quoted above then gives $v \approx 30$ m/s for HDPE at room temperature. Therefore once the dislocation has travelled a distance l_c from the free surface, it can then easily move across the lamella to produce a unit slip of b.

At large strains the model predicts that the total slipped distance across a given slip plane can be an appreciable fraction of the lamellar thickness. The slip process examined above would seem to suggest that crystallinity and the effective lamellar thickness would decrease at the large strains due to the separation of Van der Waals bonds occurring at the lamellar surface. This is not borne out by experimental observations which show crystallinity remains relatively unaltered [39]. It is proposed here that, although the actual carbon atoms involved in the crystalline and amorphous phases across a slip plane change during a relative displacement of b, the microstructure of the crystalline phase remains the same size in terms of effective lamellar thickness, d, and total crystallinity (Fig. 6).

Wu *et al.* [40] used small angle neutron scattering to examine the deformation of blends of protonated and deuterated polyethylene. They demonstrated that the deuterated polyethylene fraction was partially segregated in the undeformed state but became more evenly distributed after plastic deformation. They used their results as validation for a partial melting-recrystallisation process. The process proposed here accommodates these results since parts of molecular chains can move from the amorphous to crystalline phase and vice versa.

4.2. Rate constant of the slip process

Krausz and Eyring [25] describe the absolute rate theory for thermally activated reactions passing over a free enthalpy barrier ΔG. The forward reaction is defined to be in the direction of the applied stress and the reaction rate as the number of transformations per unit volume over the energy barrier. The reaction passes over a potential barrier and a *complex* which has obtained enough energy to pass over this barrier is said to be in the activated state. The term *complex*, as used here, denotes the group of partial molecular chains within a lamellae that may, given sufficient thermal energy, form a stable screw dislocation as described by Equation 6. Using Boltzmann statistics to evaluate the rate, k_f, at which a given complex passes over an energy barrier in the forward direction gives:

$$k_f = \frac{\bar{v}_f}{\Delta} \exp\left(-\frac{\Delta G_{max}}{kT}\right) \tag{7}$$

The average forward velocity of the activated complexes moving within the distance Δ between stable states is $\bar{v}_f$. Eyring treats Δ as being a function of temperature. In this case the distance can be identified as the Burger's vector, b. The mean velocity of the activated complexes along the metastable degree of vibrational freedom is given by Kausz and Eyring as:

$$\bar{v}_f = \left(\frac{kT}{2\pi m_e}\right)^{\frac{1}{2}}$$

where k is the Boltzmann constant, T is the absolute temperature and m_e, the effective mass of the activated complex, is given by Kocks *et al.* [38] as approximately:

$$m_e = db^2\rho_c$$

calculated from the kinetic energy component of a dislocation moving at a constant velocity and assuming the dislocation energy is $1/2\mu b^2$. Substituting into Equation 7 gives:

$$k_f = \frac{1}{b^2}\left(\frac{kT}{2\pi d\rho_c}\right)^{\frac{1}{2}} \exp\left(-\frac{\Delta G_{max}}{kT}\right)$$

It is normal to assume the forward barrier is small compared to backward and that the backward rate can be ignored. For the model described here there are situations where this assumption cannot be made since τ_θ can fall to zero due to orientation effects. The approximation is made that the energy barrier in the back direction is given by:

$$\Delta G_{max}(l^*) = \frac{\mu db^2}{4\pi}\ln(2l^*) + \tau_\theta\, db^2 l^*$$

The above equation is only quantitatively true when $\tau_\theta \to 0$ but this is the only point at which the term is significant.

The nett forward reaction rate is therefore:

$$k_s = k_f - k_b = \frac{2}{b^2}\left(\frac{kT}{2\pi d\rho_c}\right)^{\frac{1}{2}} \exp\left(-\frac{\mu db^2}{4\pi kT}\ln(2l^*)\right) \times \sinh\left(\frac{db^2 l^*\tau_\theta}{kT}\right) \tag{8}$$

Hydrostatic pressure dependence is significant in polyethylene [41]. The dependence is due to the hydrostatic pressure straining the Van der Waals bonds and reducing the shear modulus. For the case considered here it is the normal stress, σ_n, which controls this straining. Assuming a linear dependency gives:

$$\mu = \mu_0 - \alpha\sigma_n$$

Where μ_0 is the shear modulus when $\sigma_n = 0$ and α is the hydrostatic dependency factor. The value of both μ_0 and α must be determined from experimental results but, since the data collected so far does not allow an accurate determination of α, the hydrostatic pressure dependency is not incorporated into Equation 8 at present.

Hinton and Rider [41] demonstrated the validity of using continuum mechanics to resolve shear stresses acting on slip planes at a microstructural level in polyethylene. More recently Bartczak *et al.* [28] performed more comprehensive experiments which confirmed these results.

For a Poisson's ratio of 0.5, continuum mechanics gives the shear stress (τ_θ), in uni-axial tension, on an inclined plane as:

$$\tau_\theta = \tfrac{1}{2}\sigma_{zz}\sin(2\theta)$$

where θ is the angle between this plane and the z axis and σ_{zz} is the normal stress on planes normal to the axis of extension (z). Substituting into Equation 8 gives:

$$k_s = \frac{2}{b^2}\left(\frac{kT}{2\pi d\rho_c}\right)^{\frac{1}{2}} \exp\left(-\frac{\mu_0 v_0}{4\pi kT}\frac{\ln(2l^*)}{l^*}\right) \times \sinh\left(\frac{v_0\sigma_{zz}\sin(2\theta)}{2kT}\right) \quad (9)$$

where the activation volume, $v_0 = db^2l^*$.

4.3. Slip strain

To complete the model, the relationship between macroscopic strain and the rate constant given by Equation 9 must be determined. The first step is to decide how lamellae of different orientations interact so that the strain can be partitioned between them. Before describing the interaction law a 'composite unit' is defined as the crystalline material surrounding a single slip plane together with the neighbouring amorphous material associated with it.

To remain true to the pseudo-affine model the composite units are forced to act in parallel to form an aggregate. The total normal stress on the aggregate is then the sum of the individual normal stresses on each composite unit in the aggregate. In extreme cases of slip unit orientation (0°, ±90° and 180°) the resolved shear stress will be zero. Without including any alternative deformation to slip, these cases would lead to an infinitely high normal stress under an imposed finite strain. This is physically unrealistic, the strain being accommodated by bond or chain stretching or the initiation of higher energy slip systems. The composite unit is therefore modelled as an elastic and viscous element in series, as in the Maxwell model. The viscous element is associated with the slip plane only. The elastic element is associated with the material of the slip and amorphous components and is simply described by a Young's modulus, E (Fig. 7). The approach of modelling the slip units acting in parallel to form an aggregate is analogous to Ward's aggregate model using Voigt averaging [42].

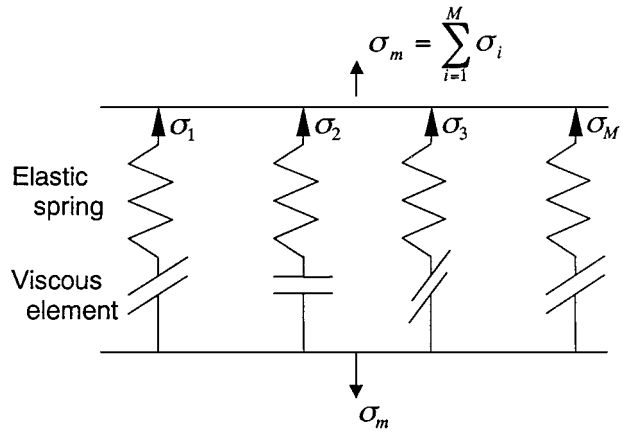

Figure 7 Array of composite units arranged in parallel to form an aggregate.

His aggregate model also incorporated pseudo-affine deformation to describe reorientation of the molecular chains. The primary purpose of Ward's model was to describe the anisotropic development of modulus due to drawing, which has been neglected here. Instead, the present model concentrates on the slip process to show how it can explain the hardening behaviour observed in experiments. However, due to the similarity with Ward's model, it would be relatively straightforward to include the stiffening characteristics he proposed.

The simplest approach to quantify the slip strain is to examine a representative slip plane as shown in Fig. 8. Small angle and wide angle X-ray scattering results [29, 31] show that the normals to a lamellar surface rotate away from the chain direction as a result of fine chain slip. The spacing between slip planes, a_0, is therefore taken as the average {h,k,0} plane spacing (0.493 nm). The representative axial length of the plane is then:

$$l_i = \frac{a_0}{\sin(\theta_i)}$$

The rate of change of length due to slip is given by:

$$\dot{l}_i = bk_s\cos(\theta_i)$$

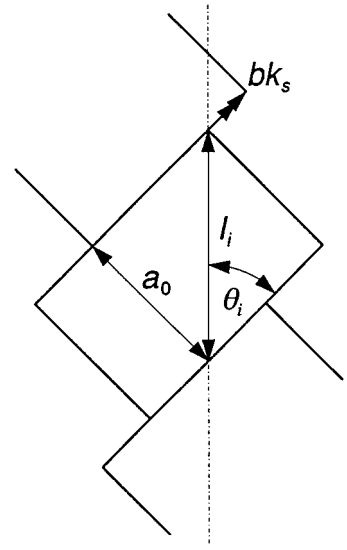

Figure 8 Slip strain due to a slip unit.

The true strain-rate due to slip is therefore:

$$\dot{\varepsilon}_i^{\mathrm{s}} = \frac{\dot{l}_i}{l_i} = \frac{b}{2a_0} k_{\mathrm{s}} \sin(2\theta_i) \tag{10}$$

The true strain-rate due to elastic extension is given by:

$$\dot{\varepsilon}_i^{\mathrm{e}} = \frac{\dot{\sigma}_i}{E} \tag{11}$$

where E is the Young's modulus.

The sum of the slip and elastic components of extension rate is equal to the strain rate on the aggregate:

$$\dot{\varepsilon}_{\mathrm{m}} = \dot{\varepsilon}_i^{\mathrm{e}} + \dot{\varepsilon}_i^{\mathrm{s}} \tag{12}$$

Substituting for the individual strain rates from Equation 10 and gives a differential equation in σ_i which can be numerically integrated over time to give the stress-stretch response of each composite unit. The total true stress on the aggregate can then be calculated by summing the contributions from each unit.

4.4. Crystallinity

Up until this point total crystallinity has not been accounted for. Young [43] proposed that the shear stress is supported only by the crystalline fraction but this has not been incorporated into the model since a main assumption is that the amorphous phase can support a significant stress. From the viewpoint of the model proposed here, the main effect is the reduction in Young's modulus of the composite unit with decreasing crystallinity. Kennedy *et al.* [44] demonstrated that E is in fact better characterised by the thickness of the inter lamellar amorphous phase but this thickness is itself dependent on crystallinity.

5. Model predictions and characteristics

This section compares the predictions of the model to true stress strain data, measured at constant true strain-rate measured by Hillmansen *et al.* [4] for the bimodal high-density polyethylene described above. The only unknown parameters in the model are μ, E and l^*. The modulus, E, was set to give the correct initial slope of the stress strain curve. Its value was altered with test temperature but *not* test rate. The values used are shown in Fig. 9.

The approximate dependency of true stress on true strain-rate for any given orientation is shown more clearly if the derived value of k_{s} from Equation 9 is substituted into Equation 12 and k_{b}, $\dot{\varepsilon}^{\mathrm{e}}$ are assumed to be negligible:

$$\sigma_i \left(\sin(2\theta_i) + \alpha \frac{\ln(2l^*)}{2\pi l^*} \sin^2(\theta_i) \right) = \frac{\ln(2l^*)}{2\pi l^*} \mu_0 + \frac{2kT}{v_0} \ln\left(\dot{\varepsilon}_i^{\mathrm{s}}\right) - \frac{2kT}{v_0} \ln\left(\dot{\varepsilon}_i^{0}\right) \tag{13}$$

where

$$\dot{\varepsilon}_0 = \frac{\sin(2\theta_i)}{2ba_{\mathrm{o}}} \left(\frac{kT}{2\pi d \rho_{\mathrm{c}}} \right)^{\frac{1}{2}}$$

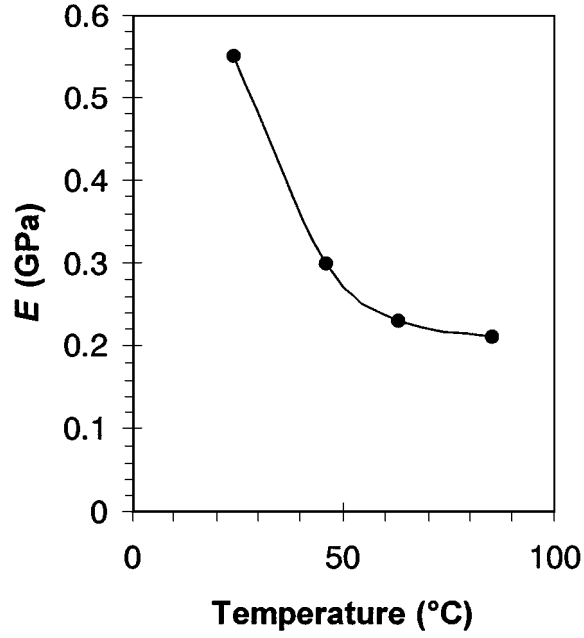

Figure 9 Values of composite modulus, E, used in the model for each temperature.

The activation volume, $v_0 = db^2 l^* = 5.6$ nm^3, was set to give the measured strain-rate sensitivity. The approximate lamellar thickness, d, in HDPE is 20 nm which gives a value of l^* as 4.34.

The predicted temperature sensitivity is dependent on both the strain-rate constant ($\dot{\varepsilon}_0$) and the crystal shear modulus (μ_0). The theoretical value of the crystal shear modulus is 3.4 GPa at 24°C falling by only 0.25 GPa to 3.15 GPa at 85°C. Due to the uncertainty in the quantitative accuracy of the free energy calculation (Equation 3), μ_0 is treated here as a calibration constant independent of temperature in order to maintain clarity. In this manner μ_0 was found to be 0.7 GPa. The effective mass calculation used in evaluating the strain-rate constant is only approximate but gives satisfactory results, as can be seen from the temperature dependence shown in Fig. 2. The model does not predict the correct hardening at high temperatures and strains. This could be due to two reasons:

- Firstly, the hydrostatic pressure sensitivity, α, defined in section 4.2 has been neglected due to insufficient data. In reality, at high strains, the energy required to nucleate an edge dislocation would be higher due to the crystal shear modulus increasing as the normal stress decreases.
- Secondly, the elastic modulus of the composite units becomes higher at high strains due to alignment of the molecular chains. To demonstrate this effect in a crude way the prediction of the model at 24°C and 85°C is shown in Fig. 10 with exactly the same parameter values as above but for an increase in elastic modulus by a factor of 10 (2.1 GPa and 5.5 GPa at 24°C and 85°C respectively). As can be seen a much better agreement with experiment occurs at high strains, the effect being more pronounced at high temperatures due to the ease of slip.

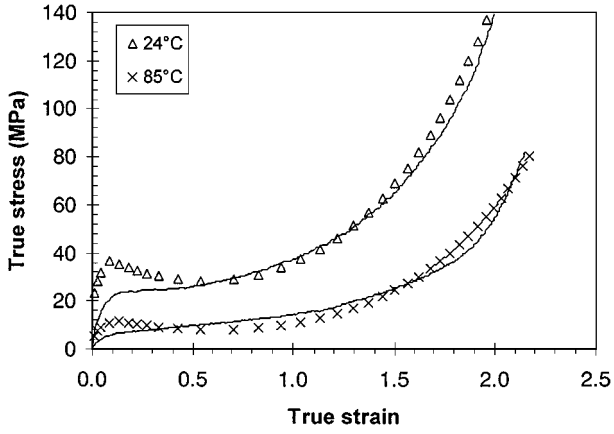

Figure 10 Experimental and predicted true stress strain results as shown in Fig. 2 but for an increase in composite modulus, E, by a factor of 10.

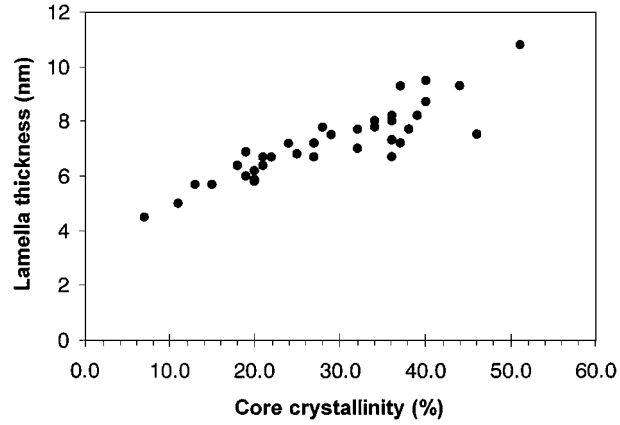

Figure 11 Lamellar thickness as a function of core crystallinity from the data of Kennedy *et al.* [44].

6. Discussion

The model presented here captures most of the main characteristics of the true stress-strain characteristic of an HDPE. The model indicates how these characteristics depend on microstructural parameters. The parallel combination of elements has a similarity to creep models. As such the model should be of use in examining stress-relaxation data since the pseudo-affine model is also valid for this case [10].

The model has been kept to a bare minimum of complexity. The main areas which are seen as providing the most significant improvements are given below:

- Ward's model for the development of anisotropy of the modulus can be included to produce a sharper upturn in the stress-strain curve at high strains. A further improvement might be obtained by using rubber elasticity theory to model the amorphous phase.
- As the temperature is increased above 70°C the crystalline units start to melt at an increasing rate, increasing the partial chain lengths in the amorphous regions and reducing the modulus. The effect can be largely modelled by calibrating the dependence of μ and E on temperature. However, the average lamellar thickness, which must increase due to the lower stability of small thickness lamellae, might also have to be accounted for.

It is often the case that molecular characteristics such as molecular weight and branch content are investigated with regard to their effect on mechanical properties such as yield stress. The model presented above provides a convenient stepping stone between these two types properties via a material's microstructural properties. For example, Kennedy *et al.* [44] demonstrated that although the yield stress initially increases with lamellar thickness it becomes less sensitive at high lamellar thicknesses. The model predictions agree with this result. Kennedy *et al.* also used Young's proposal that only the crystalline phase supports the yield stress to show that the critical resolved shear stress on the lamellae is not dependent on lamellar thickness. However, from the viewpoint of the model presented here, which does not support Young's proposal, the critical resolved shear stress is dependent on lamellar thickness. Therefore one arrives at the conclusion that lamellar thickness must be proportional to crytallinity. Fig. 11 was generated from the data of Kennedy *et al.* to demonstrate the validity of this conclusion.

The zero spin condition for uni-axial tension in simulations based on the Taylor model is automatically satisfied in this model due to axial symmetry of the slip lines. For the cases where the distribution is not isotropic, or the deformation is not restrained by the zero spin condition the results of Hinton and Rider on pre-oriented specimens indicate that the model can still provide satisfactory predictions.

The model shows that, although a molecular chain's entropy must be reducing as it orientates towards the draw direction, entropic forces are not necessarily the dominant cause of the hardening observed. This is substantiated by tests performed in shear, which show that there is little or no hardening [45]. The shear result can be explained by reorientation causing the slip planes to become aligned with the plane of maximum shear stress.

Acknowledgements

The author gratefully acknowledges the many discussions with Mr P. Davis and Dr P. S. Leevers. The work was funded by a grant awarded from the EPSRC.

References

1. S. J. K. RITCHIE, P. DAVIES and P. S. LEEVERS, *Polymer* **39** (1998) 6657.
2. R. HISS and G. STROBL, in Proc. 10th International Conference on Deformation Yield and Fracture of Polymers (Institute of Materials, London, 1997) p. 439.
3. C. G'SELL and J. J. JONAS, *J. Mater. Sci.* **14** (1979) 583.
4. S. HILLMANSEN, S. HOBEIKA, R. N. HAWARD and P. S. LEEVERS, *Polymer Engineering and Science* **40** (2000) 481.
5. R. N. HAWARD and G. THACKRAY, *Proc. Roy. Soc. London* **A302** (1968) 453.
6. M. C. BOYCE, D. M. PARKS and A. S. ARGON, *Int. J. Plasticity* **5** (1989) 593.
7. L. R. G. TRELOAR, "The Physics of Rubber Elasticity" (Oxford University Press, London, 1949).
8. C. G'SELL and J. J. JONAS, *J. Mater. Sci* **16** (1981) 1956.
9. R. N. HAWARD, *Macromolecules* **26** (1993) 5860.

10. S. M. CRAWFORD and H. KOLSKY, *Proc. Phys. Soc. B* **64** (1951) 119.
11. S. AHZI, B. J. LEE and R. J. ASARO, *Mater. Sci. and Eng* **A189** (1994) 35.
12. C. G'SELL and A. DAHOUN, *ibid.* **A175** (1994) 183.
13. S. K. KHAN and S. HUANG, "Continuum Theory of Plasticity" (John Wiley & Sons Inc, New York, 1995).
14. W. KUHN and F. GRÜN, *Kolloidzschr.* **101** (1942) 248.
15. A. S. MAXWELL, A. P. UNWIN and I. M. WARD, *Polymer* **37** (1996) 3283.
16. Z. BARTCZAK, A. GALESKI, A. S. ARGON and R. E. COHEN, *Polymer* **37** (1996) 2113.
17. N. BROWN and I. M. WARD, *J. Mater. Sci.* **18** (1983) 1405.
18. R. G. VADIMSKY, H. D. KEITH and F. J. PADDEN, *J. Polymer Sci. part A-2* **7** (1969) 1367.
19. P. J. FLORY and D. Y. YOON, *Nature* **272** (1978) 226.
20. R. ALAMO, R. DOMSZY and L. MANDELKERN, *J. Phys. Chem.* **88** (1984) 6587.
21. P. SCHOUTERDEN, G. GROENINCKX, B. VAN DER HEIJDEN and F. JANSEN, *Polymer* **28** (1987) 2099.
22. H. SCHÖNHERR, G. J. VANCSO and A. S. ARGON, *ibid.* **36** (1995) 2115.
23. J. W. S. HEARLE, "Polymers and their Properties, Volume 1: Fundamentals of Structure and Mechanics" (Ellis Horwood Ltd, Chichester, 1982).
24. M. F. BUTLER, A. M. DONALD and J. R. RYAN, in Proc. 10th International Conference on Deformation Yield and Fracture of Polymers (Institute of Materials, London, 1997) p. 41.
25. A. S. KRAUSZ, H. EYRING, "Deformation Kinetics" (John Wiley and Sons, New York, 1975).
26. B. CRIST, in "The Physics of Glassy Polymers," edited by R. N. Howard and R. J. Young (Chapman and Hall, London, 1997).
27. Z. BARTCZAK, A. S. ARGON and R. E. COHEN, *Polymer* **35** (1994) 3427.
28. *Idem., Macromolecules* **25** (1992) 5036.
29. R. J. YOUNG, P. B. BOWDEN, J. M. RITCHIE and J. G. RIDER, *J. Mater. Sci.* **8** (1973) 23.
30. L. G. SHADRAKE and F. GUIU, *Phil. Mag.* **34** (1976) 565.
31. A. GALESKI, Z. BARTCZAK, A. S. ARGON and R. E. COHEN, *Macromolecules* **25** (1992) 5705.
32. H. GLEITER and A. S. ARGON, *Phil. Mag.* **24** (1971) 71.
33. R. J. YOUNG, *ibid.* **30** (1974) 85.
34. J. M. PETERSON, *J. Appl. Phys.* **37** (1966) 4047.
35. L. LIN and A. S. ARGON, *J. Mater. Sci.* **29** (1994) 294.
36. J. FRIEDEL, in "Dislocations," edited by R. Smoluchowski and N. Kurti (Pergamon, Oxford, 1964).
37. J. O. ESHELBY and A. N. STROH, *Phil. Mag.* **42** (1951) 1401.
38. U. F. KOCKS, A. S. ARGON and M. F. ASHBY, "Progress in Materials Sci," edited by B. Chalmers, J. W. Christian and T. B. Massaloki (Pergamonn, Oxford, 1975).
39. P. DAVIS, PhD thesis, University of London (1999).
40. W. WU, G. D. WIGNALL and L. MANDELKERN, *Polymer* **33** (1992) 4137.
41. T. HINTON and J. G. RIDER, *J Appl. Phys.* **39** (1968) 4932.
42. I. M. WARD and D. W. HADLEY, "An Introduction to the Mechanical Properties of Solid Polymers" (John Wiley and Sons Ltd, Chichester, 1993).
43. R. J. YOUNG, *Mater. Forum* **11** (1988) 210.
44. M. A. KENNEDY, A. J. PEACOCK, M. D. FAILLA, J. C. LUCAS and L. MANDELKERN, *Macromolecules* **28** (1995) 1407.
45. C. G'SELL, S. BONI and S. SHRIVASTASA, *J. Mater. Sci.* **18** (1983) 903.

Received 21 December 1999
and accepted 27 April 2000